

Dirac quasinormal frequencies of Reissner-Nordström black hole in Anti-de Sitter spacetime

Jiliang Jing and Qiyuan Pan*

*Institute of Physics and Department of Physics,
Hunan Normal University,
Changsha, Hunan 410081, P. R. China*

Abstract

The quasinormal modes (QNMs) of Dirac field perturbations of a Reissner-Nordström black hole in an asymptotically Anti-de Sitter spacetime are investigated. We find that both the real and imaginary parts of the fundamental quasinormal frequencies for large black holes are the linear functions of the Hawking temperature, and the slope of the lines for the real parts decreases while that for the magnitude of the imaginary parts increases as the black hole charge increases. According to the Anti-de Sitter/Conformal Field Theory (AdS/CFT) correspondence, the fact shows that different charge presents different time scale in three-dimensional CFT. Another interesting result is that the quasinormal frequencies become evenly spaced for high overtone number, and in the spacing expressions the real part decreases while the magnitude of the imaginary part increases as the charge increases. We also study the relation between quasinormal frequencies and angular quantum number and find that the real part increases while the magnitude of the imaginary part decreases as the angular quantum number increases.

PACS numbers: 04.70.-s, 04.50.+h, 11.15.-q, 11.25.Hf

*Electronic address: jljing@hunnu.edu.cn

I. INTRODUCTION

It is well known that QNMs possess discrete spectra of complex characteristic frequencies which are entirely fixed by the structure of the background spacetime and are irrelevant of the initial perturbations [1] [2]. Thus, it is believed that one can directly identify a black hole existence by comparing QNMs with the gravitational waves observed in the universe, as well as test the stability of the event horizon against small perturbations. Meanwhile, it is generally believed that the study of QNMs may lead to a deeper understanding of the thermodynamic properties of black holes in loop quantum gravity [3] [4] since the real part of quasinormal frequencies with a large imaginary part for the scalar field in the Schwarzschild black hole is equal to the Barbero-Immirzi parameter [3][4] [5][6], a factor introduced by hand in order that the loop quantum gravity reproduces correct entropy of the black hole.

Motivated by the AdS/CFT correspondence, the study of QNMs in AdS spacetime becomes appealing recently. It was argued that the QNMs of AdS black holes have a direct interpretation in terms of the dual conformal field theory [7] [8] [9]. According to the AdS/CFT correspondence, a large static black hole in asymptotically AdS spacetime corresponds to an (approximately) thermal state in CFT, and the decay of the test field in the black hole spacetime corresponds to the decay of the perturbed state in CFT. The dynamical timescale for the return to the thermal equilibrium can be done in AdS spacetime, and then translated onto the CFT, using the AdS/CFT correspondence. The QNMs in AdS spacetime were first computed for a conformally invariant scalar field by Chan and Mann [10]. Subsequently, Horowitz and Hubeny [11] presented a numerical method to evaluate the quasinormal frequencies directly and made a systematic investigation of QNMs for the scalar field in the Schwarzschild AdS black hole. Then, many authors studied QNMs for the scalar, electromagnetic and gravitational perturbations in various asymptotically AdS black holes [12] -[24]. Although QNMs for the scalar, electromagnetic and gravitational field perturbations in the Schwarzschild AdS and the Reissner-Nordström AdS black-hole backgrounds have been investigated extensively, QNMs for the Dirac field perturbations in the Schwarzschild AdS black hole were first studied in Refs. [25][26] recently. Considering the Reissner-Nordström AdS (RNAdS) black hole spacetime provides a better background than the Schwarzschild AdS geometry, in this paper we will extend the study in Ref. [26] to the RNAdS black hole and see how the black hole charge affects the Dirac QNMs.

The organization of this paper is as follows. In Sec.2 the decoupled Dirac equations and the corresponding wave equations in the RNAdS spacetime are obtained by using Newman-Penrose formalism. In Sec.3 the numerical approach to compute the Dirac QNMs is introduced. In Sec.4 the numerical results for the Dirac QNMs in the RNAdS black hole are presented. The last section is devoted to a summary.

II. DIRAC EQUATIONS IN THE REISSNER-NORDSTRÖM ANTI-DE SITTER SPACETIME

The line element of the RNAdS black hole can be expressed as

$$ds^2 = f dt^2 - \frac{1}{f} dr^2 - r^2(d\theta^2 + \sin^2\theta d\varphi^2), \quad (2.1)$$

with

$$f = 1 - \frac{2M}{r} + \frac{Q^2}{r^2} + \frac{r^2}{R^2}, \quad (2.2)$$

where M , Q and R represent the mass, charge and anti-de Sitter radius, respectively. Hereafter we will take $R = 1$ and measure everything in terms of R . The spacetime causal structure depends on the zeros of f . Changing the parameters M and Q , the function f may have none, one or two positive zeros. In general case, f has two simple real, positive roots r_- and r_+ , but in the so-called extreme case, f has one double positive zero r_+ (because $r_- = r_+$). The horizons r_- and r_+ with $r_- < r_+$, are called Cauchy and event horizons respectively. The Hawking temperature of the black hole is given by

$$T_H = \frac{\kappa}{2\pi} = \frac{1 - Q^2/r_+^2 + 3r_+^2}{4\pi r_+}, \quad (2.3)$$

where κ is the surface gravity. The mass parameter M is related to the charge Q and the event horizon radius r_+ by the relation

$$M = \frac{1}{2} \left(r_+ + r_+^3 + \frac{Q^2}{r_+} \right), \quad (2.4)$$

and the extremal value of the black hole charge, Q_{ext} , is given by

$$Q_{ext}^2 = r_+^2 (1 + 3r_+^2). \quad (2.5)$$

In a curved spacetime the Dirac equations [27] are described by

$$\begin{aligned} \sqrt{2}\nabla_{BB'}P^B + i\mu\bar{Q}_{B'} &= 0, \\ \sqrt{2}\nabla_{BB'}Q^B + i\mu\bar{P}_{B'} &= 0, \end{aligned} \quad (2.6)$$

where $\nabla_{BB'}$ is covariant differentiation, P^B and Q^B are the two-component spinors representing the wave function, $\bar{P}_{B'}$ is the complex conjugate of P_B , and μ is the particle mass. In order to separate the Dirac equations in the RNAdS spacetime (2.1) by using Newman-Penrose formalism [28], we take the null tetrad as

$$\begin{aligned} l^\mu &= \left(\frac{r^2}{\Delta}, 1, 0, 0 \right), \\ n^\mu &= \frac{1}{2} \left(1, -\frac{\Delta}{r^2}, 0, 0 \right) \\ m^\mu &= \frac{1}{\sqrt{2}r} \left(0, 0, 1, \frac{i}{\sin\theta} \right), \end{aligned} \quad (2.7)$$

with

$$\Delta = r^2 - 2Mr + Q^2 + r^4, \quad (2.8)$$

and set the two-component spinors as

$$\begin{aligned} P^0 &= \frac{1}{r} \mathbb{R}_{-1/2} S_{-1/2} e^{-i(\omega t - m\varphi)}, \\ P^1 &= \mathbb{R}_{+1/2} S_{+1/2} e^{-i(\omega t - m\varphi)}, \\ \bar{Q}^{1'} &= \mathbb{R}_{+1/2} S_{-1/2} e^{-i(\omega t - m\varphi)}, \\ \bar{Q}^{0'} &= -\frac{1}{r} \mathbb{R}_{-1/2} S_{+1/2} e^{-i(\omega t - m\varphi)}, \end{aligned} \quad (2.9)$$

where $\mathbb{R}_{+1/2}$ and $\mathbb{R}_{-1/2}$ are functions of the coordinate r , and $S_{+1/2}$ and $S_{-1/2}$ are functions of the coordinate θ . Following the steps in Refs. [26, 29], after the tedious calculation we find that the Dirac equations can be reduced to the following radial and angular parts

$$\sqrt{\Delta} \mathcal{D}_0 \mathbb{R}_{-1/2} = (\lambda + i\mu r) \sqrt{\Delta} \mathbb{R}_{+1/2}, \quad (2.10)$$

$$\sqrt{\Delta} \mathcal{D}_0^\dagger (\sqrt{\Delta} \mathbb{R}_{+1/2}) = (\lambda - i\mu r) \mathbb{R}_{-1/2}, \quad (2.11)$$

$$\mathcal{L}_{1/2} S_{+1/2} = -\lambda S_{-1/2}, \quad (2.12)$$

$$\mathcal{L}_{1/2}^\dagger S_{-1/2} = \lambda S_{+1/2}, \quad (2.13)$$

with

$$\begin{aligned} \mathcal{D}_n &= \frac{\partial}{\partial r} - \frac{iK}{\Delta} + \frac{n}{\Delta} \frac{d\Delta}{dr}, \\ \mathcal{D}_n^\dagger &= \frac{\partial}{\partial r} + \frac{iK}{\Delta} + \frac{n}{\Delta} \frac{d\Delta}{dr}, \\ \mathcal{L}_n &= \frac{\partial}{\partial \theta} + \frac{m}{\sin \theta} + n \cot \theta, \\ \mathcal{L}_n^\dagger &= \frac{\partial}{\partial \theta} - \frac{m}{\sin \theta} + n \cot \theta, \\ K &= r^2 \omega. \end{aligned} \quad (2.14)$$

We can eliminate $S_{+1/2}$ (or $S_{-1/2}$) from Eqs. (2.12) and (2.13) and obtain

$$\left[\frac{1}{\sin \theta} \frac{d}{d\theta} \left(\sin \theta \frac{d}{d\theta} \right) - \frac{m^2 + 2m s \cos \theta + s^2 \cos^2 \theta}{\sin^2 \theta} + s + A_s \right] S_s = 0, \quad (2.15)$$

where $A_{+1/2} = \lambda^2 - 1$ and $A_{-1/2} = \lambda^2$. The angular equation (2.15) can be solved exactly and $A_s = (l - s)(l + s + 1)$, where l is the quantum number characterizing the angular distribution. Thus, for both cases $s = \pm 1/2$ we have

$$\lambda^2 = \left(l + \frac{1}{2} \right)^2. \quad (2.16)$$

In what follows, we focus our attention on the massless Dirac field. Then, we can eliminate $\mathbb{R}_{-1/2}$ (or $\mathbb{R}_{+1/2}$) from Eqs. (2.10) and (2.11) to obtain a radial decoupled Dirac equation for $\mathbb{R}_{+1/2}$ (or $\mathbb{R}_{-1/2}$), and we find that both them can be expressed as

$$\Delta^{-s} \frac{d}{dr} \left(\Delta^{1+s} \frac{d\mathbb{R}_s}{dr} \right) + P\mathbb{R}_s = 0, \quad (2.17)$$

with

$$P = \frac{K^2 - isK \frac{d\Delta}{dr}}{\Delta} + 4si\omega r + \frac{1}{2} \left(s + \frac{1}{2} \right) \frac{d^2\Delta}{dr^2} - \lambda^2. \quad (2.18)$$

Introducing an usual tortoise coordinate

$$dr_* = (r^2/\Delta)dr, \quad (2.19)$$

and resolving the equations in the form

$$\mathbb{R}_s = \frac{\Delta^{-s/2}}{r} \Psi_s, \quad (2.20)$$

we obtain

$$\frac{d^2\Psi_s}{dr_*^2} + (\omega^2 - V)\Psi_s = 0, \quad (2.21)$$

where

$$V = -\frac{\Delta}{4r^2} \frac{d}{dr} \left[r^2 \frac{d}{dr} \left(\frac{\Delta}{r^4} \right) \right] + \frac{s^2 r^4}{4} \left[\frac{d}{dr} \left(\frac{\Delta}{r^4} \right) \right]^2 + is\omega r^2 \frac{d}{dr} \left(\frac{\Delta}{r^4} \right) + \frac{\lambda^2 \Delta}{r^4}. \quad (2.22)$$

The potential V is complex and the complex frequency ω is not separated from the potential. As many authors [30] [31] [32] [33] have found that such complex potential can also present correct quasinormal frequencies provided we use proper boundary conditions.

III. NUMERICAL APPROACH

The QNMs of AdS black holes are usually defined as the solutions of the relevant wave equations characterized by purely ingoing waves at the black hole event horizon and vanishing of the perturbation at the radial infinity. Therefore, the boundary conditions on wave function Ψ_s (or \mathbb{R}_s) at the event horizon ($r = r_+$) and the radial infinity ($r \rightarrow \infty$) can be mathematically expressed as

$$\Psi_s \sim \Delta^{s/2} \mathbb{R}_s \sim \begin{cases} \Delta^{-s/2} e^{-i\omega r_*} & r \rightarrow r_+, \\ 0 & r \rightarrow \infty. \end{cases} \quad (3.1)$$

Equations (2.21), (2.22) and (3.1) determine an eigenvalue problem for the quasinormal frequency ω of the Dirac field perturbations.

We will calculate the quasinormal frequencies for outgoing Dirac field (i.e., for the case $s = -1/2$ [30]) by using the Horowitz-Hubeny approach [11]. Writing Φ_s for a generic wave function as

$$\Phi_s = \Psi_s e^{i\omega r_*}, \quad (3.2)$$

then, Eq. (2.21) can be rewritten as

$$f^2 \frac{d^2 \Phi_s}{dr^2} + \left(f \frac{df}{dr} - 2i\omega f \right) \frac{d\Phi_s}{dr} - V \Phi_s = 0. \quad (3.3)$$

To map the entire region of interest, $r_+ < r < +\infty$, into a finite parameter range, we change variable to $x = 1/r$. Define a new function $B(x)$ as

$$B(x) = x^2 - \frac{1 + x_+^2 + Q^2 x_+^4}{x_+^3} x^3 + Q^2 x^4 + 1, \quad (3.4)$$

then f can be rescaled as

$$f = x^2 \Delta = \frac{B(x)}{x^2}. \quad (3.5)$$

In terms of the new variable x , Eq. (3.3) can be expressed as

$$S(x) \frac{d^2 \Phi_s}{dx^2} + \frac{T(x)}{x - x_+} \frac{d\Phi_s}{dx} + \frac{U(x)}{(x - x_+)^2} \Phi_s = 0, \quad (3.6)$$

where

$$\begin{aligned} S(x) &= \frac{B(x)^2}{(x - x_+)^2} = \left(\frac{1 + x_+^2}{x_+^3} x^2 + \frac{x}{x_+^2} + \frac{1}{x_+} - Q^2 x^3 \right)^2, \\ T(x) &= \frac{B(x)}{x - x_+} \left(\frac{dB(x)}{dx} + 2i\omega \right) \\ &= \left(\frac{1 + x_+^2}{x_+^3} x^2 + \frac{x}{x_+^2} + \frac{1}{x_+} - Q^2 x^3 \right) \left(\frac{3(1 + x_+^2 + Q^2 x_+^4)}{x_+^3} x^2 - 2x - 4Q^2 x^3 - 2i\omega \right), \\ U(x) &= -V = \frac{B(x)}{4} \frac{d^2 B(x)}{dx^2} - \frac{s^2}{4} \left(\frac{dB(x)}{dx} \right)^2 + is\omega \frac{dB(x)}{dx} - \lambda^2 B(x). \end{aligned} \quad (3.7)$$

We can expand $S(x)$ about the event horizon $x = x_+$ as $S(x) = \sum_{n=0}^6 S_n (x - x_+)^n$ since $S(x)$ is a polynomial of degree 6, and similarly for $T(x)$ and $U(x)$.

In order to evaluate the quasinormal frequencies by using the Horowitz-Hubeny method, we need to expand the solution to the wave function Φ_s around x_+ ,

$$\Phi_s = (x - x_+)^{\alpha} \sum_{k=0}^{\infty} a_k (x - x_+)^k. \quad (3.8)$$

It is easy to show that the index α has two solutions $\alpha = -\frac{s}{2}$ and $\alpha = \frac{s}{2} + \frac{i\omega}{\kappa}$. Because we need only the ingoing modes near the event horizon, that is to say, Φ_s must satisfy the boundary condition (3.1), we take $\alpha = -\frac{s}{2}$. Then Φ_s becomes

$$\Phi_s = (x - x_+)^{-s/2} \sum_{k=0}^{\infty} a_k (x - x_+)^k. \quad (3.9)$$

Substituting Eq. (3.9) into Eq. (3.6) we find the following recursion relation for a_n

$$a_n = -\frac{1}{Z_n} \sum_{k=0}^{n-1} \left[\left(k - \frac{s}{2}\right) \left(k - \frac{s}{2} - 1\right) S_{n-k} + \left(k - \frac{s}{2}\right) T_{n-k} + U_{n-k} \right] a_k, \quad (3.10)$$

where $Z_n = 4n\kappa[(n-s)\kappa - i\omega]$.

The boundary condition (3.1) at $r \rightarrow \infty$ becomes

$$\sum_{k=0}^{\infty} a_k (-x_+)^k = 0. \quad (3.11)$$

Now the computation of quasinormal frequencies is reduced to find roots of the Eq. (3.11). We truncate the sum (3.11) at some large $k = N$ and then check that for greater k the roots converge to some true roots, i.e., quasinormal frequencies. In the series (3.10) and (3.11) each next term depends on all the preceding terms through the recursion relations, and the roots of (3.11) suffer a sharp change for a small change on any of the input parameters, especially for finding the higher overtone modes. In order to avoid the “noisy” we increase the precision of all the input data and retain 70-digital precision in all the intermediate process.

IV. NUMERICAL RESULTS

In this section we represent the numerical results obtained by using the numerical procedure just outlined in the previous section. The results will be organized into four subsections: the fundamental QNMs, dependence of the black hole charge, higher modes, and dependence of the angular quantum number.

A. Fundamental Quasinormal Modes

The fundamental quasinormal frequencies ($n = 0$) corresponding to $\lambda = 1$ Dirac perturbation for RNAdS black holes ($r_+ = 5, 10, 25, 50, 75, 100$) with the charge $Q = 0, 0.1Q_{ext}, 0.3Q_{ext}, 0.5Q_{ext}$ are given by table (I) and corresponding results are drawn in Fig. (1). From the table and figures we find that, for the large black holes, both the real and

TABLE I: The fundamental quasinormal frequencies ($n = 0$) corresponding to $\lambda = 1$ Dirac perturbation of the RNAdS black holes ($r_+ = 5, 10, 25, 50, 75, 100$) with the charge $Q = 0, 0.1Q_{ext}, 0.3Q_{ext}, 0.5Q_{ext}$.

r_+	$\omega(Q = 0)$	$\omega(Q = 0.1Q_{ext})$	$\omega(Q = 0.3Q_{ext})$	$\omega(Q = 0.5Q_{ext})$
100	199.769-152.016i	198.415-153.628i	187.351-169.030i	182.694-217.611i
75	149.834-114.012i	148.817-115.220i	140.519-126.770i	137.024-163.204i
50	99.8993-76.0043i	99.2226-76.8101i	93.6914-84.5094i	91.3576-108.796i
25	49.9795-37.9952i	49.6411-38.3968i	46.8775-42.2439i	45.7003-54.3789i
10	20.0744-15.1751i	19.9398-15.3357i	18.8398-16.8675i	18.3406-21.6987i
5	10.1834-7.54760i	10.1173-7.62708i	9.57673-8.38092i	9.27945-10.7551i

the imaginary parts of the quasinormal frequencies are the linear functions of the Hawking temperature, and the lines are described by

$$\begin{aligned}
Re(\omega(Q = 0)) &= 8.367T, \\
Re(\omega(Q = 0.1Q_{ext})) &= 8.309T, \\
Re(\omega(Q = 0.3Q_{ext})) &= 7.845T, \\
Re(\omega(Q = 0.5Q_{ext})) &= 7.652T,
\end{aligned} \tag{4.1}$$

and

$$\begin{aligned}
-Im(\omega(Q = 0)) &= 6.371T, \\
-Im(\omega(Q = 0.1Q_{ext})) &= 6.439T, \\
-Im(\omega(Q = 0.3Q_{ext})) &= 7.084T, \\
-Im(\omega(Q = 0.5Q_{ext})) &= 9.121T,
\end{aligned} \tag{4.2}$$

which show that the slope of the lines for the real parts decreases as the charge increases, but the slope of the lines for the magnitude of the imaginary parts increases as the charge increases.

According to the AdS/CFT correspondence, the decay of the Dirac perturbation can be translated into a time scale for the approach to the thermal equilibrium in CFT. The time scale is simply given by the imaginary part of the lowest quasinormal frequency, $\tau = 1/|Im(\omega)|$.

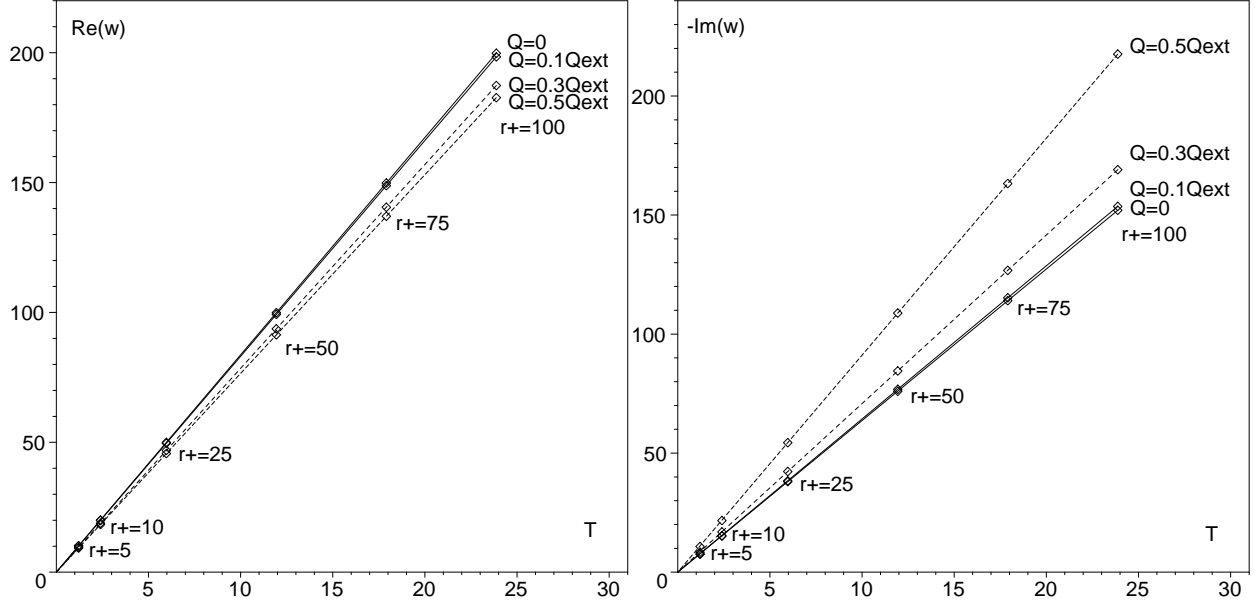


FIG. 1: Graphs of fundamental quasinormal frequencies ω versus the Hawking temperature T for black holes ($r_+ = 5, 10, 25, 50, 75, 100$) with $\lambda = 1$. The left figure is drawn for $Re(\omega)$ in which the lines from the top to the bottom correspond to $Q = 0, 0.1Q_{ext}, 0.3Q_{ext}, 0.5Q_{ext}$, and the right one for $Im(\omega)$ in which the lines from the top to the bottom correspond to $Q = 0.5Q_{ext}, 0.3Q_{ext}, 0.1Q_{ext}, 0$. The figures show that both the real and the imaginary parts of the frequencies are the linear functions of T .

From Eqs. (4.2) we know that for three-dimensional CFT the time scales are

$$\begin{aligned}
 \tau(Q = 0) &= 0.1570/T, \\
 \tau(Q = 0.1Q_{ext}) &= 0.1553/T, \\
 \tau(Q = 0.3Q_{ext}) &= 0.1412/T, \\
 \tau(Q = 0.5Q_{ext}) &= 0.1096/T,
 \end{aligned}
 \tag{4.3}$$

which show that different black hole charge presents different time scale.

B. Dependence on the black hole charge

The relation between the quasinormal frequencies and the charges of the black hole for $n = 0, 1, 3, 5, r_+ = 100$ and $\lambda = 1$ is shown by Fig. (2). We know from figures for $Re(\omega)$ with Q/Q_{ext} in Fig. (2) that the local minima of the “wiggles” appear as the scalar and gravitational perturbations [16][34]. The “wiggles” become shallower as the overtone number n increases and disappears for $n \geq 5$. However, we should point out that the curves of $Re(\omega)$ versus Q/Q_{ext}

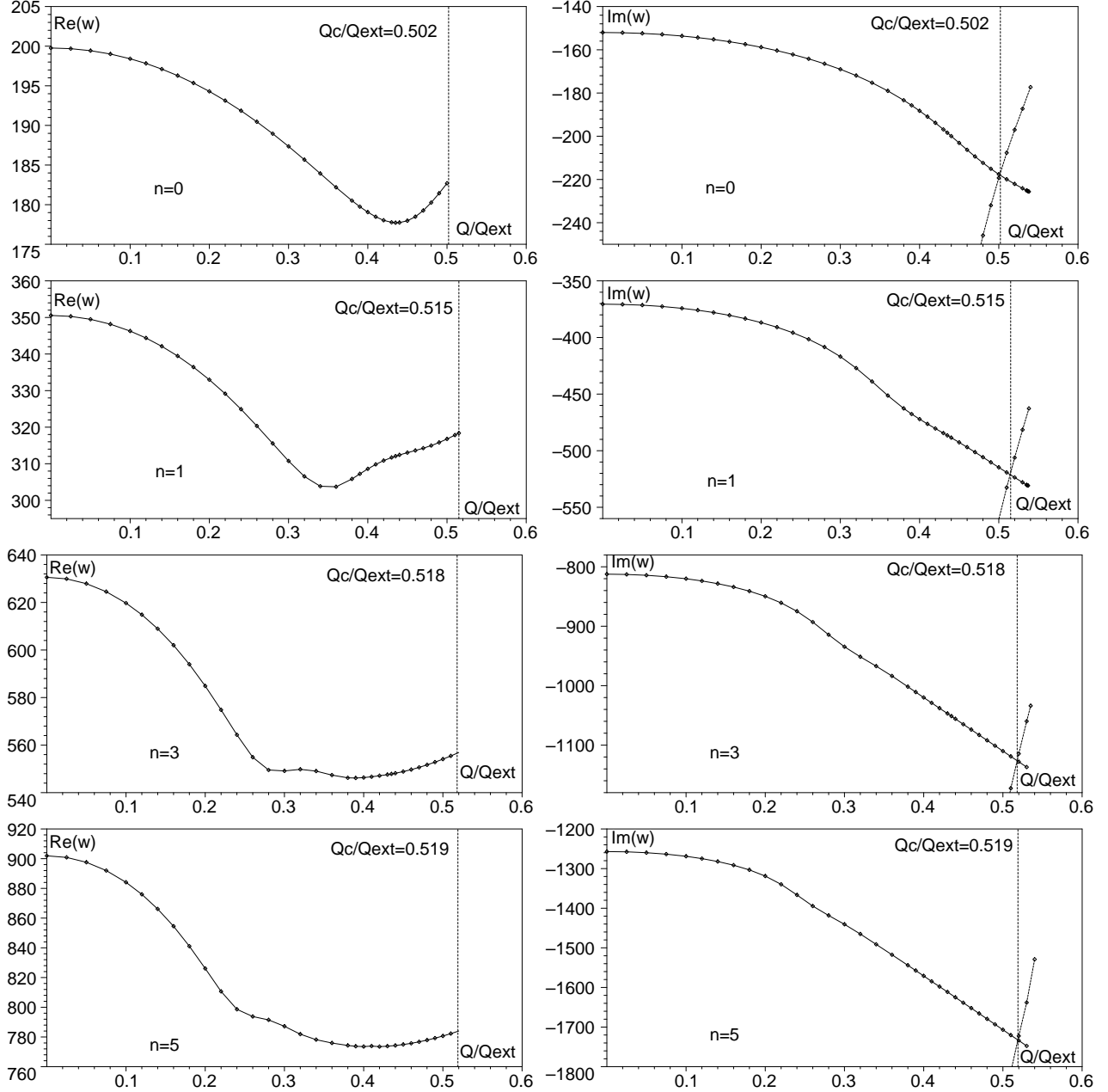


FIG. 2: Graphs of ω with Q/Q_{ext} for $n = 0, 1, 3, 5$, $r_+ = 100$ and $\lambda = 1$. The left four figures are drawn for $Re(\omega)$ which show the “wobble behavior”. The right figures for $Im(\omega)$ in which the continuous lines describe the oscillatory modes and the dashed lines indicate the non-oscillatory modes. Values of Q_c/Q_{ext} in the graphs indicate when non-oscillating dominates.

for the Dirac field are different from those of the scalar field and gravitational perturbations [16][34].

The figures for $Im(\omega)$ versus Q/Q_{ext} in Fig. (2) tell us that there are two stable classes of solutions for QNMs when the value of the charge nears Q_c , i. e., the oscillatory modes

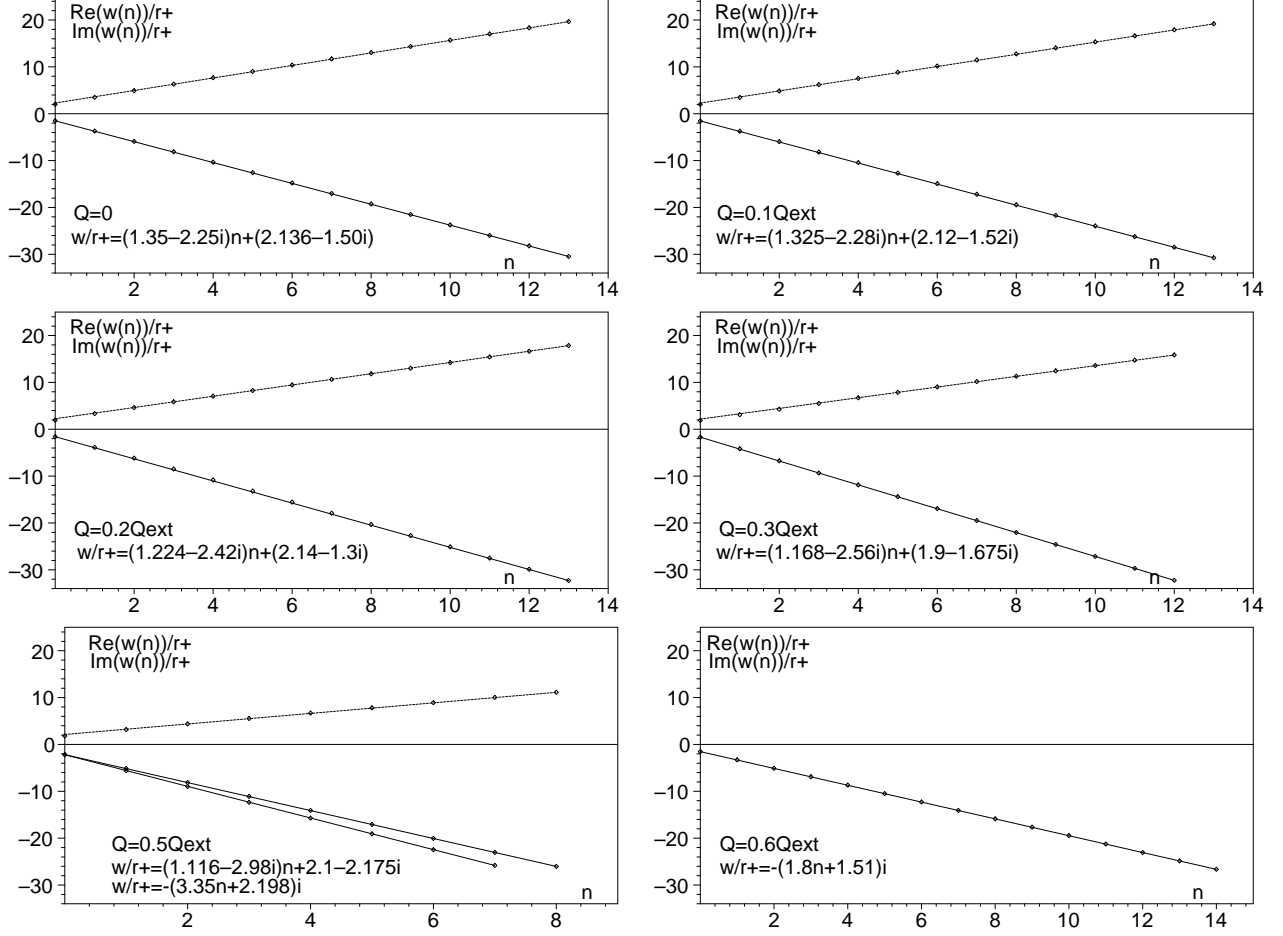


FIG. 3: Graphs of $\frac{\omega(n)}{r_+}$ versus n corresponding to $\lambda = 1$ Dirac perturbations of a large RNAdS black hole ($r_+ = 100$) for $Q = 0, 0.1Q_{ext}, 0.2Q_{ext}, 0.3Q_{ext}, 0.5Q_{ext}, 0.6Q_{ext}$. The dashed lines describe $\frac{Re(\omega(n))}{r_+}$ and the solid lines are $\frac{Im(\omega(n))}{r_+}$. It is interesting to note that the quasinormal frequencies become evenly spaced for high overtone number n .

(the frequencies have both the real and imaginary parts) and the non-oscillatory modes (the frequencies are purely imaginary). For the RNAdS black holes with the charge $Q < Q_c$, the Dirac perturbation decay is dominated by oscillatory modes. But for the black holes with the charge $Q > Q_c$, the decay is dominated by non-oscillatory modes. The figures also show us that the value of the critical value of the charge Q_c slightly increases as the overtone number n increases.

C. Higher modes

In Fig. (3) we graph $\frac{\omega(n)}{r_+}$ versus n corresponding to $\lambda = 1$ Dirac perturbations of a large RNAdS black hole ($r_+ = 100$) for $Q = 0, 0.1Q_{ext}, 0.2Q_{ext}, 0.3Q_{ext}, 0.5Q_{ext}, 0.6Q_{ext}$. The

behavior of the QNMs can be written as $\frac{\omega(n)}{r_+} \sim (1.35 - 2.25i)n + (2.136 - 1.50i)$ for $Q=0$, $\frac{\omega(n)}{r_+} \sim (1.325 - 2.28i)n + (2.12 - 1.52i)$ for $Q = 0.1Q_{ext}$, $\frac{\omega(n)}{r_+} \sim (1.224 - 2.42i)n + (2.14 - 1.30i)$ for $Q = 0.2Q_{ext}$, $\frac{\omega(n)}{r_+} \sim (1.168 - 2.56i)n + (1.90 - 1.675i)$ for $Q = 0.3Q_{ext}$, $\frac{\omega(n)}{r_+} \sim (1.116 - 2.98i)n + (2.1 - 2.175i)$ and $-(3.35n + 2.198)i$ for $Q = 0.5Q_{ext}$, $\frac{\omega(n)}{r_+} \sim -(1.8n + 1.51)i$ for $Q = 0.6Q_{ext}$.

Cardoso et al [19] found that the scalar quasinormal frequencies for the large Schwarzschild-AdS black hole become evenly spaced for high overtone number n . Our results extend their argument to the Dirac quasinormal frequencies of the RNAdS black hole for fixed value of the charge. The spacings between frequencies are given by

$$\begin{aligned}
\frac{\omega(n+1) - \omega(n)}{r_+} &\sim (1.35 - 2.25i) && \text{for } Q = 0, \\
\frac{\omega(n+1) - \omega(n)}{r_+} &\sim (1.325 - 2.28i) && \text{for } Q = 0.1Q_{ext}, \\
\frac{\omega(n+1) - \omega(n)}{r_+} &\sim (1.224 - 2.42i) && \text{for } Q = 0.2Q_{ext}, \\
\frac{\omega(n+1) - \omega(n)}{r_+} &\sim (1.168 - 2.56i) && \text{for } Q = 0.3Q_{ext}, \\
\frac{\omega(n+1) - \omega(n)}{r_+} &\sim (1.116 - 2.98i) && \\
&\sim (\quad - 3.35i) && \text{for } Q = 0.5Q_{ext}.
\end{aligned} \tag{4.4}$$

From which we find that, for lowly charged RNAdS black hole, the real part in the spacing expression decreases as the charge increases, while the magnitude of the imaginary part increases as the charge increases.

It is obvious that there are two stable classes of solutions for the QNMs with $Q = 0.5Q_{ext}$. In the first class the frequencies have both the real and imaginary parts (oscillatory modes), and in the second class the frequencies are purely imaginary (non-oscillatory modes). But there is only an oscillatory mode for the case with the small charge (say $Q = 0.1Q_{ext}$), and there is only a non-oscillatory modes for the case with the large charge (say $Q = 0.6Q_{ext}$).

D. Dependence on the angular quantum number

We also study the relation between the quasinormal frequencies and the angular quantum number l and the results are presented in figure (4). We learn from the figures that the $Re(\omega)$ increases (decreases the oscillatory time scale) and $|Im(\omega)|$ decreases (increases the damping time scale) as the angular quantum number l increases for fixed n , though quasinormal frequencies depend very weakly on l . Besides, the figures tell us that for the imaginary parts $|dW|$ increases as the charge Q increases. We also find that the larger the overtone number n ,

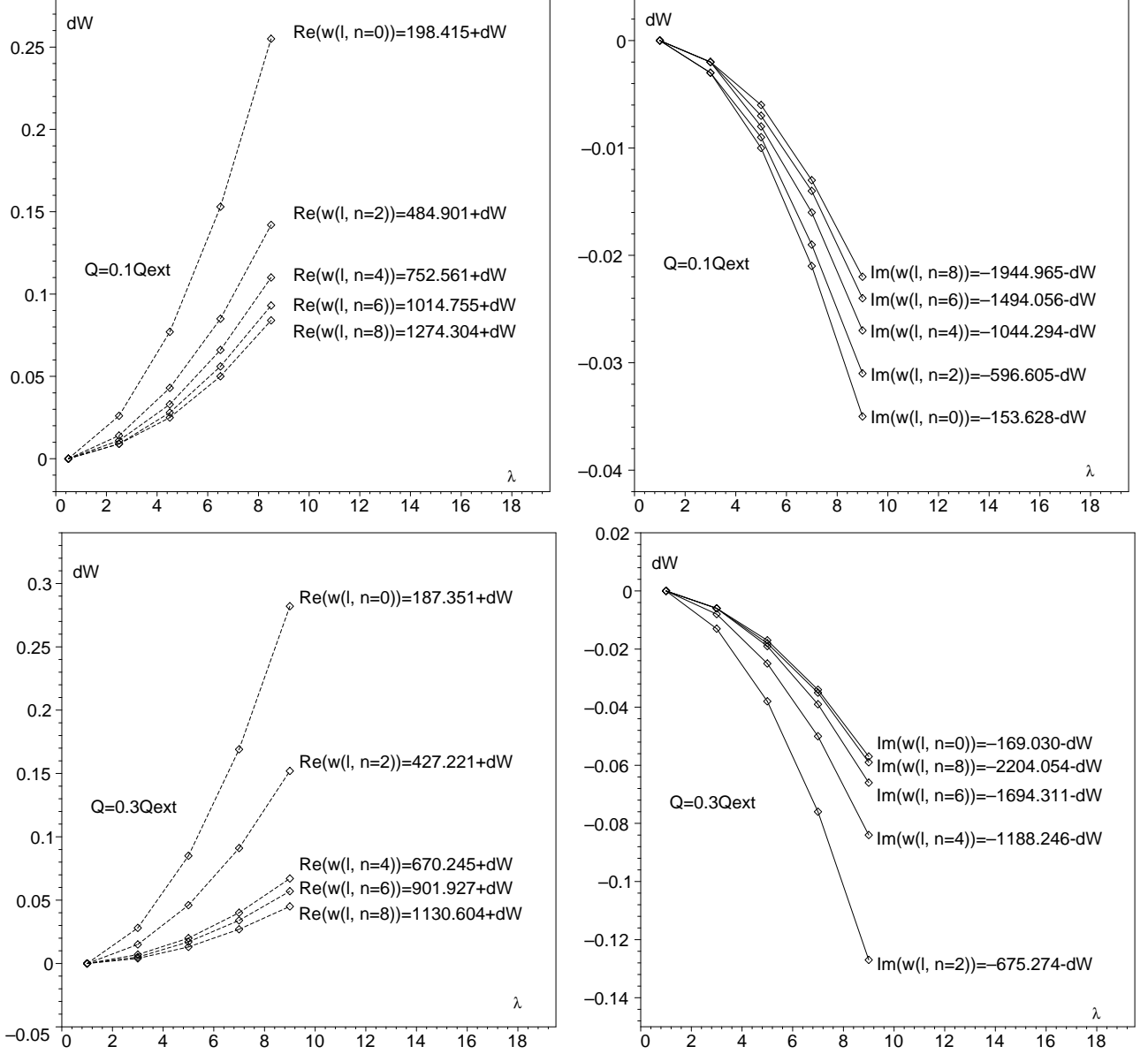


FIG. 4: Graphs of the increment dW with λ (or l) for several value of $n = 0, 2, 4, 6, 8$ and $Q = 0.1Q_{ext}, 0.3Q_{ext}$. The left two figures are drawn for $dW = \text{Re}(\omega(l, n)) - \text{Re}(\omega(0, n))$ and the right two are for $dW = -\text{Im}(\omega(l, n)) + \text{Im}(\omega(0, n))$. The figures show that $\text{Re}(\omega)$ increases and $|\text{Im}(\omega)|$ decreases with increase of l for fixed n , though the dependence is very weak. Besides, the figures tell us that the larger the value of the charge Q , the larger the increment $|dW|$ for the imaginary parts. We also find that the larger the overtone number n , the smaller the increment $|dW|$ except for the case of $\text{Im}(\omega(l, n = 0))$ with $Q = 0.3Q_{ext}$.

the smaller the increment $|dW|$ except for the case of $Im(\omega(l, n = 0))$ with $Q = 0.3Q_{ext}$.

V. SUMMARY

The Dirac fields in the RNAdS black hole spacetime are separated by means of the Newman-Penrose formulism. Then, the quasinormal frequencies corresponding to the Dirac field perturbations are studied by using the Horowitz-Hubeny approach and the results are presented by table and figures. We have shown that: (i) Both the real and the imaginary parts of the fundamental quasinormal frequency for the RNAdS black holes ($r_+ = 5, 10, 25, 50, 75, 100$) with the charge $Q = 0, 0.1Q_{ext}, 0.3Q_{ext}, 0.5Q_{ext}$ are the linear functions of the Hawking temperature. The slope of the lines for the real parts decreases as the charge increases, but the slope for the magnitude of the imaginary parts increases as the charge increases. According to the AdS/CFT correspondence, the decay of the Dirac perturbation can be translated into a time scale for the approach to the thermal equilibrium in CFT. The time scale is simply given by the imaginary part of the lowest quasinormal frequency, $\tau = 1/|Im(\omega)|$. Thus, for three-dimensional CFT the time scales are $\tau = 0.1570/T, 0.1553/T, 0.1412/T, 0.1096/T$ for $Q = 0, 0.1Q_{ext}, 0.3Q_{ext}, 0.5Q_{ext}$, respectively, which show that different charge presents different time scale. (ii) There are two stable classes of QNMs when the value of the charge nears Q_c , i. e., the oscillatory modes and the non-oscillatory modes. The Dirac perturbation decay is dominated by the oscillatory modes for the black hole with the charge $Q < Q_c$, but the decay is dominated by the non-oscillatory modes for the black hole with the charge $Q > Q_c$. The value of the critical value of the charge Q_c slightly increases as the overtone number n increases. (iii) The Dirac quasinormal frequencies of the large RNAdS black holes become evenly spaced for high overtone number n . For lowly charged RNAdS black hole, the real part in the spacing expression decreases as the value of the charge increases, while the magnitude of the imaginary part increases as the charge increases. (iv) The $Re(\omega)$ increases (decreases the oscillatory time scale) and $|Im(\omega)|$ decreases (increases the damping time scale) as the angular quantum number l increases for fixed n , though quasinormal frequencies depend very weakly on l .

Acknowledgments

This work was supported by the National Natural Science Foundation of China under Grant No. 10275024 and under Grant No. 10473004; the FANEDD under Grant No. 200317; and

the SRFDP under Grant No. 20040542003.

- [1] S. Chandrasekhar and S. Detweiler, Proc. R. Soc. Lond. **A 344**, 441 (1975).
- [2] V. P. Frolov and I. D. Novikov, Black hole physics: basic concepts and new developments (Kluwer Academic, Dordrecht, 1998).
- [3] S. Hod, Phys. Rev. Lett. **81**, 4293 (1998).
- [4] O. Dreyer, Phys. Rev. Lett. **90**, 081301 (2003).
- [5] J. Baez, in Matters of gravity. ed. J. Pullin, p. 12(Springer, 2003), gr-qc/0303027.
- [6] G. Kunstatter, gr-qc/0212014; L. Motl, gr-qc/0212096; A. Corichi, gr-qc/0212126; L. Motl and A. Neitzke, hep-th/03301173; A. Maassen van den Brink, gr-qc/0303095.
- [7] J. Maldacena, Adv. Theor. Math. Phys. **2**, 231 (1998).
- [8] E. Witten, Adv. Theor. Math. Phys. **2**, 253 (1998).
- [9] S. Kalyana Rama and Sathiapalan, Mod Phys. Lett. A **14**, 2635 (1999).
- [10] J. S. F. Chan and R. B. Mann, Phys. Rev. D **55**, 7546 (1997); **59**, 064025 (1999).
- [11] G. T. Horowitz and V. E. Hubeny, Phys. Rev. D **62**, 024027 (2000).
- [12] V. Cardoso and J. P. S. Lemos, Phys. Rev. D **64**, 084017 (2001).
- [13] V. Cardoso, R. Konoplya and J. P. S. Lemos, gr-qc/0305037.
- [14] R. A. Konoplya, Phys. Rev. D **66**, 044009 (2002).
- [15] B. Wang, C. Y. Lin and E. Abdalla, Phys. Lett. B **481**, 79 (2000).
- [16] B. Wang, C. Y. Lin and C. Molona, hep-th/0407024.
- [17] I. G. Moss and J. P. Norman, Class. Quantum Grav. **19**, 2323 (2002).
- [18] D. Birmingham, I. Sachs and S. N. Solodukhin, Phys. Rev. Lett. **88**, 151301 (2002).
- [19] V. Cardoso and J. P. S. Lemos, Phys. Rev. D **63**, 124015 (2001).
- [20] A. O. Starinets, Phys. Rev. D **66**, 124013 (2002).
- [21] R. Aros, C. Martinez, R. Troncoso and J. Zanelli, Phys. Rev. D **67**, 044014 (2003).
- [22] R. A. Konoplya, Phys. Rev. D **66**, 084007 (2002).
- [23] A. Nunez and A. O. Starinets, Phys. Rev. D **67**, 124013 (2002).
- [24] Y. Kurita and M. A. Sakagami, Phys. Rev. D **67**, 024003 (2003).
- [25] M. Giammatteo and Jiliang Jing, gr-qc/0403030.
- [26] Jiliang Jing, submitted to Phys. Rev. D .

- [27] D. N. Page, Phys. Rev. D **14**, 1509 (1976).
- [28] E. Newman and R. Penrose, J. Math. Phys. (N. Y.) **3**, 566 (1962).
- [29] Jiliang Jing, Phys. Rev. D **70**, 065004 (2004).
- [30] E. W. Leaver, Phys. Rev. D **34**, 384 (1986).
- [31] K. D. Kokkotas, Class. Quantum Grav. **8**, 2217 (1991).
- [32] H. T. Cho, Phys. Rev. D **68**, 024003 (2003).
- [33] L. Simone and C. M. Will, class. Quantum Grav. **9**, 963 (1992).
- [34] E. Berti and K. D. Kokkotas, Phys. Rev. D **67**, 064020 (2003).